

## Absence of ferromagnetism in epitaxial films of ultrathin Pd, Rh, and Rh on Pd grown on Au(100)

C. Liu and S. D. Bader

*Materials Science Division, Argonne National Laboratory, Argonne, Illinois 60439*

(Received 24 June 1991)

*In situ* longitudinal and polar Kerr-effect measurements were used to search for ferromagnetism in films of Pd/Au(100), Rh/Au(100), and Rh/Pd/Au(100) with overlayer thicknesses of 0.5–5 monolayers (ML). No evidence for ferromagnetism was found in these systems above 100 K and for applied magnetic fields up to 2.2 kOe. Based on our low-energy-electron-diffraction and Auger data, we find that all three systems grow epitaxially, and that there is layer-by-layer growth for Pd/Au(100) at 300 K, layer growth for Rh/Au(100) at 100 K up to 2 ML followed by island formation, and layer growth for Rh/Pd/Au(100) at 100 K.

Ultrathin transition-metal films have received much attention recently because of their unusual magnetic properties.<sup>1,2</sup> A striking prediction of computational physics that has motivated the experimental surface-magnetism community is of ordered moments in monolayers of elements that are paramagnetic in bulk form.<sup>3</sup> A prime example is of monolayer vanadium grown pseudomorphically on Ag(100) for which the experimental search has led to conflicting reports that either refute<sup>4,5</sup> or confirm<sup>6</sup> the prediction.<sup>3</sup> Recently, the magnetic properties of monolayers of heavy 4*d* metals were examined computationally by a number of researchers because of the likelihood of discovering ferromagnetic instabilities which occur in the heavy 3*d* metals. Eriksson, Albers, and Boring<sup>7</sup> investigated the total energy of pseudomorphic Tc, Ru, Rh, and Pd overlayers on Ag(100), and concluded that monolayer Rh/Ag(100) has a ferromagnetic ground state with a magnetic moment of  $0.6\mu_B$ , while Ru/Ag(100) shows several metamagnetic states very close in energy to the paramagnetic state, and that Tc and Pd are paramagnetic. Li<sup>8</sup> summarizes his results for Ru, Rh, and Pd monolayers by reporting that only his square lattice of Ru exhibits ferromagnetism, with a moment of  $\sim 0.8\mu_B$ , but that the ordering is not stable when the Ru is on Ag(100). Zhu, Bylander, and Kleinman<sup>9</sup> treated Pd(100) both as a free-standing monolayer at the Ag(100) lattice spacing, and also as an overlayer on Ag(100), and found moments of 0.4 and  $0\mu_B$ , respectively. Zhu, Bylander, and Kleinman<sup>10</sup> also treated Rh(100) both as a free-standing monolayer, and as an overlayer on Au(100), and found moments of 1.56 and  $1.09\mu_B$ , respectively. They also explored the possibility of an antiferromagnetic instability and ruled it out. Pd seems like a particularly interesting candidate because in its bulk form it is near a ferromagnetic instability.<sup>11</sup> Moruzzi and Marcus<sup>12</sup> predicted a first-order transition at expanded volume for bulk Pd to a ferromagnetic state with a moment that can exceed  $0.3\mu_B$ . Jarlborg and Freeman<sup>13</sup> predicted a high-field metamagnetic state for bulk Pd with a moment of  $0.19\mu_B$ . Blügel *et al.*<sup>14</sup> have calculated induced moments of  $0.3\mu_B$  for the interfacial layer of Pd when Pd(100) serves as a substrate for 3*d*-magnetic overlayers. Despite the motivation, Fink *et al.*<sup>5</sup> were unsuccessful in their search for ferromagnetism in Pd/Ag(100). In the present work we use the sur-

face magneto-optic Kerr-effect SMOKE combined with low-energy-electron-diffraction (LEED) and Auger growth studies to search for ferromagnetism in monolayers of Pd, Rh, and Pd/Rh grown on Au(100). We find epitaxy and predominantly layer-by-layer growth, but no ferromagnetic hysteresis in the Kerr loops, which should have adequate sensitivity for the task.

The Au(100) substrate was prepared by mechanical and electrochemical polishing followed by cleaning in ultrahigh vacuum (UHV) using repeated Ar<sup>+</sup> sputter-anneal cycles. The UHV base pressure was  $8 \times 10^{-11}$  Torr. Homoepitaxial evaporation of Au was used to smooth the Au(100) surface. No detectable impurities were found via Auger spectroscopy using a double-pass cylindrical mirror analyzer. LEED patterns showed the typical  $(5 \times 20)$  reconstruction characteristic of a clean Au(100) surface,<sup>15</sup> as shown in Fig. 1(a), in which the two orthogo-

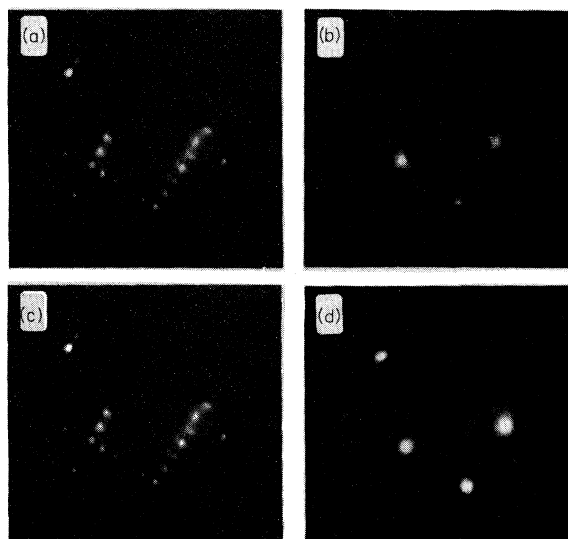


FIG. 1. LEED patterns for (a) the  $(5 \times 20)$ -reconstructed surface of clean Au(100); (b)  $\sim 3$  ML of Pd on Au(100) at 300 K; (c)  $\sim 3$  ML of Rh on Au(100) at 100 K; and (d)  $\sim 2$  ML of Rh grown on  $\sim 10$  ML Pd/Au(100) at 100 K and annealed at 450 K. All patterns were recorded at room temperature and at an electron-beam energy of  $\sim 66$  eV.

nal domains give rise to fivefold splittings along each of the two principal axes. Pd was grown on Au(100) at 300 K at a rate of  $\sim 1$  ML/min from a resistive evaporator made by winding a pure Pd wire on a W spiral. During the evaporation the vacuum stabilized at  $< 5 \times 10^{-10}$  Torr. Upon deposition of Pd, the  $(5 \times 20)$  reconstruction of the Au substrate transformed into a sharp  $p(1 \times 1)$  LEED pattern [Fig. 1(b)] which persisted to the thickest films grown ( $\sim 10$  ML).

It was reported previously that Pd grows on Au(100) in a layer-by-layer fashion.<sup>16</sup> In the present work the growth mode was studied by Auger peak-to-peak intensity-versus-deposition-time measurements. The data in Fig. 2(a) are well represented by exponential growth and decay curves. The data also can be fitted as straight-line segments with intersections that are equally spaced in time or dosage intervals. The linear segments would represent the discrete nature of one atomic layer attenuating the next. For an ideal layer-by-layer-growth model, the inelastic mean free path  $\lambda$  governs the exponential attenuation law of Auger signals.<sup>17</sup> The model yields a unique relationship between the slopes of the straight-line segments:  $S_3/S_1 = (S_2/S_1)^2$ , where  $S_i$  is the slope of the  $i$ th segment.<sup>18</sup> This constraint helps determine the positions where the linear segments intersect. We identify their location by arrows in Fig. 2(a), and find that  $S_3/S_1 = 0.417$  and  $(S_2/S_1)^2 = 0.418$  for the Au, and  $S_3/S_1 = 0.439$  and  $(S_2/S_1)^2 = 0.429$  for the Pd Auger data. Using the first intersection to indicate the completion of the first monolayer, we obtain  $\lambda = 5.3$  Å for the 69-eV Au and 8.3 Å for

the 330-eV Pd Auger electrons, as compared to published values of  $\lambda = 5.1$ – $5.8$  Å for Au and 9.5 Å for Pd.<sup>16</sup> Thus our  $\lambda$  values are consistent with expectation based on the “universal curve” of electron spectroscopy.<sup>19</sup> Although these results are all indicative of a layer-by-layer growth mode, we do not want to overstate the point. There are subtleties to the characterization as we learned recently in experiments to determine the morphology of ultrathin Fe/Pd(100) using photoemission from physisorbed Xe as a probe.<sup>20</sup> Our Auger studies indicated that the Fe grows on Pd(100) in a predominant layer-by-layer mode, but the Xe experiments indicated, in addition, a tendency towards a random-site-occupancy morphology in which subsequent Fe layers start to grow before the prior layers are fully occupied. Similar behavior may occur for Pd on Au(100), as indicated by the rounding of the data in Fig. 2(a) where discontinuities might otherwise occur at the intersections of the linear segments. Thus we conclude that the growth mode of Pd/Au(100) is imperfect or only nearly perfect layer-by-layer growth.

Rh was grown on Au(100), at a grazing angle of  $\sim 30^\circ$ , from a resistive evaporator made by winding a pure Rh wire on the center portion of a W filament. A quartz-crystal thickness monitor was used to check the stability of the Rh evaporator. The deposition was carried out at a reduced substrate temperature of  $\sim 100$  K at a rate of  $\sim 0.3$  ML/min and with a pressure rise to  $\sim 2 \times 10^{-9}$  Torr. Epitaxial growth was obtained despite the large lattice mismatch ( $\sim 7\%$ ) between Rh and Au. Figure 1(c) shows the LEED pattern taken at 300 K for a 3-ML Rh film grown on Au(100) at  $\sim 100$  K. Auger growth measurements again were carried out and the significant difference for Rh/Au(100) compared to Pd/Au(100) is that the Au Auger signal decreased quite slowly after the deposition of the first two monolayers of Rh. The Auger data could not be fitted to an exponential curve without an offset term. However, the data for the *initial* growth fit well with an exponential curve, as shown in Fig. 2(b). We can identify two equal-spaced segments corresponding to the growth of the first two Rh monolayers, using the same procedure as above for the Pd/Au(100). The quartz-crystal thickness monitor readings confirmed that the evaporation rate was constant, although no attempt was made to calibrate the monitor. A noticeable change in slope during the third monolayer dosage is evident in the 69-eV Au Auger data in Fig. 2(b), so only the initial slope of the third segment was used in the fitting in this case. The  $\lambda$  values obtained are 8.6 Å for the 302-eV Rh and 5.2 Å for 69-eV Au signal, in good agreement with the universal curve range of values. We believe that at 100 K the growth mode for Rh/Au(100) is predominantly layer by layer up to 2 ML followed by island formation. Island formation can be rationalized thermodynamically<sup>21</sup> as a means to minimize the total energy because Rh has a high surface free energy (2.75 vs 1.55 J/m<sup>2</sup> for Au).<sup>22</sup> The reduced substrate temperature during growth helps inhibit surface segregation of Au.

We found that Rh also grows epitaxially on Pd/Au(100) epitaxial films. Figure 1(d) shows the  $p(1 \times 1)$  LEED pattern for 2 ML of Rh grown at 100 K on an  $\sim 10$ -ML Pd film grown on Au(100) at 300 K. The sam-

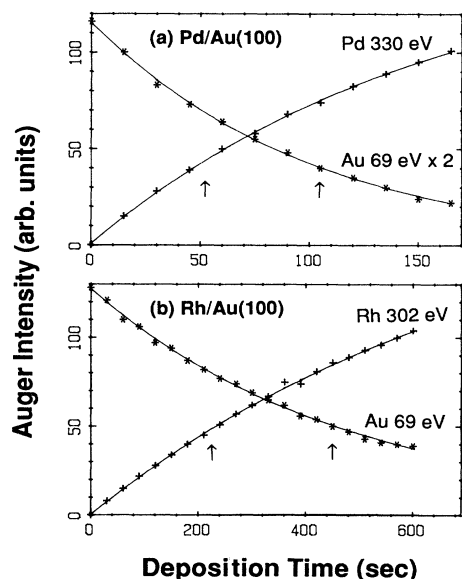


FIG. 2. Auger-intensity vs deposition-time data for (a) Pd/Au(100) grown at 300 K and (b) Rh/Au(100) grown at 100 K. The solid curves are least-squares exponential fittings of the data. The arrows point to the dosages associated with the completion of the first and second monolayers. Note that the magnitude of the 69-eV Au data at high dosage in (b) is larger than in (a), which suggests the onset of island formation for Rh/Au(100).

ple was annealed to  $\sim 450$  K for 5 min before the LEED pattern was recorded. The  $p(1 \times 1)$  pattern was observed up to 5 ML of Rh, which was the thickest film studied. Comprehensive Auger growth measurements were not carried out, although for the spectra collected the 330-eV Pd signal decreased as the 302-eV Rh signal increased.

*In situ* polar and longitudinal Kerr-effect measurements<sup>23</sup> using a He-Ne laser (wavelength 638 nm) were carried out for all three film systems: Pd/Au(100), Rh/Au(100), and Rh/Pd/Au(100). No ferromagnetic hysteresis signals were detected. The measured signals are all similar to that of the Au(100) substrate, as shown in Fig. 3, where the growth and measurement temperature was 300 K for Pd/Au(100) and 100 K for Rh/Au(100) and Rh/Pd/Au(100). We explored the Pd and Rh film-thickness range of  $\sim 0.5$ – $\sim 5$  ML, in steps of  $\sim 0.5$  ML. In addition, Rh/Au(100) and Rh/Pd/Au(100) samples were subjected to 450-K annealing, cooled in a magnetic field of  $\sim 2$  kOe, and then measured at 100 K to search for the development of ferromagnetic hysteresis.

Several possibilities must be considered before drawing any conclusions concerning the magnetism. First, our null results could indicate that the Curie temperature  $T_C$  values are below 100 K, but experimental<sup>24</sup> and theoretical<sup>25</sup> trends for  $3d$  monolayers suggest otherwise. Second, a small magneto-optical response at 638-nm wavelength could mask the magnetic signal. The response should be proportional to the moment and to a spin-orbit matrix element. Predicted  $4d$  moments are indeed lower than that of Fe, for example, but the matrix element might partially compensate for this because of the high atomic number of the  $4d$  relative to the  $3d$  elements. The vertical bars in Fig. 3 correspond to the signal we extracted previously<sup>26</sup> for 1 ML of Fe on Au(100) in the longitudinal case, and to 10% of the full signal for the polar case. The signal-to-noise level in Fig. 3 suggests we have the sensitivity to accommodate any reasonably reduced magneto-optic activity of  $4d$  ferromagnets. Third, the coercivity  $H_c$  may significantly exceed our available field, making it impossible to magnetize the films. However,  $H_c$  decreases as temperature increases,<sup>22</sup> and  $H_c$  values for monolayers in the kOe range should be limited to cryogenic temperatures. Finally, the degree of island formation at the monolayer range may be underestimated and the films might be discontinuous and superparamagnetic with a low blocking temperature compared to 100 K. Continuous overlayers would then be expected for multilayer dosages of the overlayers, but then interlayer  $4d$  hybridization may quench the magnetism. Superparamagnetic films may not be hysteretic, but they should be polarizable, and that was not observed. Thus, we conclude that our null results indicate a lack of ferromagnetism in the systems studied, at least within the confines of the search.

In summary, the LEED Auger studies indicate that

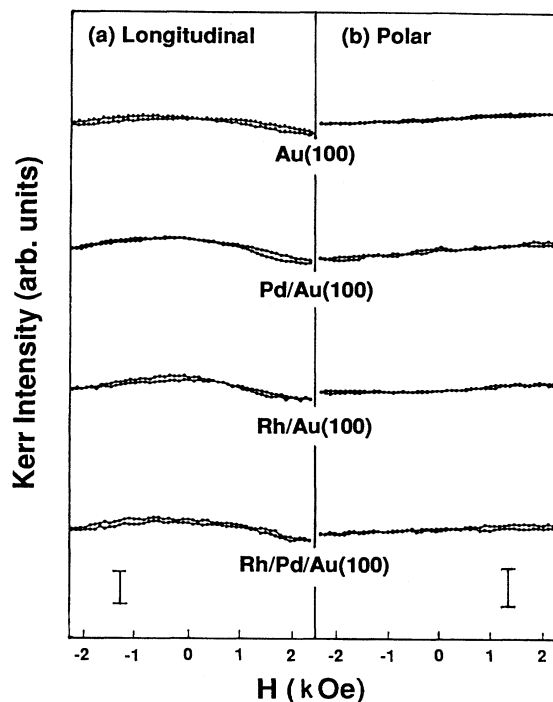


FIG. 3. (a) Typical longitudinal and (b) polar Kerr-effect signals for Au(100) at 300 K,  $\sim 3$  ML Pd/Au(100) at 300 K,  $\sim 2$  ML Rh/Au(100) at 100 K, and  $\sim 3$  ML Rh on  $\sim 10$  ML Pd/Au(100) at 100 K. No ferromagnetic signals are apparent. For comparison purposes to indicate the sensitivity of the null signals, the vertical bars in (a) indicate 100% and in (b) 10% of the full signal of a monolayer of Fe on Au(100).

each of the three ultrathin film systems studied grow epitaxially, including Pd/Au(100), Rh/Au(100), and Rh/Pd/Au(100). Pd on Au(100) grows predominantly layer by layer at 300 K at least up to 10 ML, while Rh grows in a layer-by-layer fashion up to 2 ML followed by island formation at 100 K. Three criteria were used to identify layer-by-layer growth in the Auger studies: (i) are there breaks in slope at the intersections of equally-spaced linear segments; (ii) is the slope relationship  $S_3/S_1 = (S_2/S_1)^2$  satisfied; and (iii) are the  $\lambda$  values for both overlayer and substrate Auger electrons reasonable? Most significantly, neither polar nor longitudinal Kerr-effect measurements confirmed the existence of ferromagnetism for any of the films studied.

This work was supported by the U.S. Department of Energy, BES-Materials Sciences, under Contract No. W-31-109-ENG-38. We thank J. Pearson for technical assistance.

<sup>1</sup>L. M. Falicov, D. T. Pierce, S. D. Bader, R. Gronsky, K. B. Hathaway, H. J. Hopster, D. N. Lambeth, S. S. P. Parkin, G. Prinz, M. Salamon, I. K. Schuller, and R. H. Victora, *J. Mater. Res.* **5**, 1299 (1990).

<sup>2</sup>F. Gautier, *Mater. Sci. Forum* **59 & 60**, 361 (1990).

<sup>3</sup>C. L. Fu, A. J. Freeman, and T. Oguchi, *Phys. Rev. Lett.* **54**, 2700 (1985); A. J. Freeman, and C. L. Fu, *J. Appl. Phys.* **61**, 3356 (1987).

- <sup>4</sup>M. Stampanoni, A. Vaterlaus, D. Pescia, M. Aeschlimann, F. Meier, W. Dürr, and S. Blügel, *Phys. Rev. B* **37**, 10380 (1988).
- <sup>5</sup>R. L. Fink, C. A. Ballentine, J. L. Erskine, and J. A. Araya-Pochet, *Phys. Rev. B* **41**, 10175 (1990).
- <sup>6</sup>C. Rau, G. Xing, and M. Robert, *J. Vac. Sci. Technol. A* **6**, 579 (1988).
- <sup>7</sup>O. Eriksson, R. C. Albers, and A. M. Boring, *Phys. Rev. Lett.* **66**, 1350 (1991).
- <sup>8</sup>C. Li, *Bull. Am. Phys. Soc.* **36**, 677 (1991).
- <sup>9</sup>M. J. Zhu, D. M. Bylander, and L. Kleinman, *Phys. Rev. B* **42**, 2874 (1990).
- <sup>10</sup>M. J. Zhu, D. M. Bylander, and L. Kleinman, *Phys. Rev. B* **43**, 4007 (1991).
- <sup>11</sup>M. B. Brodsky, *J. Appl. Phys.* **52**, 1665 (1981); *J. Magn. Magn. Mater.* **35**, 99 (1983).
- <sup>12</sup>V. L. Moruzzi and P. M. Marcus, *Phys. Rev. B* **39**, 471 (1989).
- <sup>13</sup>T. Jarlborg and A. J. Freeman, *Phys. Rev. B* **23**, 3577 (1981).
- <sup>14</sup>S. Blügel, M. Weinert, and P. H. Dederichs, *Phys. Rev. Lett.* **60**, 1077 (1988); S. Blügel, B. Drittler, R. Zeller, and P. H. Dederichs, *Appl. Phys. A* **49**, 547 (1989).
- <sup>15</sup>D. G. Fedak and N. A. Gjostein, *Surf. Sci.* **8**, 77 (1967); P. W. Palmberg and T. N. Rhodin, *J. Chem. Phys.* **48**, 134 (1968).
- <sup>16</sup>Y. Matsushita, K. Yagi, T. Narusawa, and G. Honjo, *Jpn. J. Appl. Phys. Suppl.* **2**, 567 (1974).
- <sup>17</sup>M. P. Seah, *Surf. Sci.* **32**, 703 (1972).
- <sup>18</sup>C. Liu, Ph.D. thesis, Simon Fraser University, 1986 (unpublished).
- <sup>19</sup>P. W. Palmberg, *Anal. Chem.* **45**, 549 (1973); C. J. Powell, *Surf. Sci.* **44**, 29 (1974).
- <sup>20</sup>C. Liu and S. D. Bader, *Phys. Rev. B* **44**, 2205 (1991).
- <sup>21</sup>E. Bauer, *Z. Krist.* **110**, 372 (1958).
- <sup>22</sup>A. R. Miedema, *Z. Metallk.* **69**, 287 (1978).
- <sup>23</sup>C. Liu, E. R. Moog, and S. D. Bader, *Phys. Rev. Lett.* **60**, 2422 (1988).
- <sup>24</sup>C. Liu and S. D. Bader, *J. Appl. Phys.* **67**, 5758 (1990).
- <sup>25</sup>K. Binder, *Thin Solid Films* **20**, 367 (1974); K. Binder and P. C. Hohenberg, *IEEE Trans. Magn.* **MAG-12**, 66 (1976).
- <sup>26</sup>C. Liu and S. D. Bader, *J. Vac. Sci. Technol.* **67**, 2727 (1990).

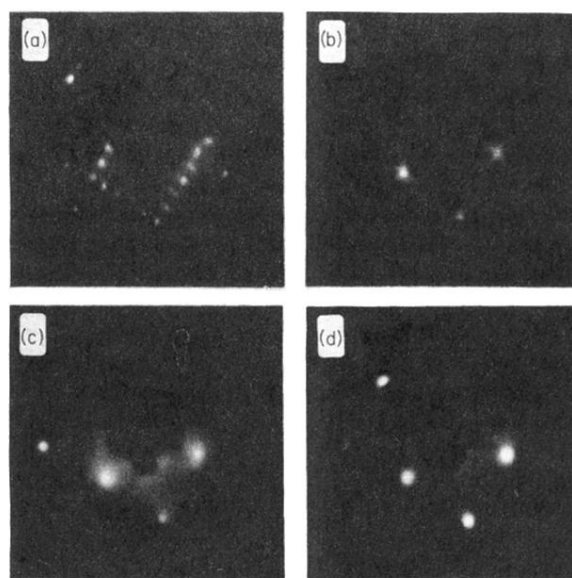


FIG. 1. LEED patterns for (a) the  $(5 \times 20)$ -reconstructed surface of clean Au(100); (b)  $\sim 3$  ML of Pd on Au(100) at 300 K; (c)  $\sim 3$  ML of Rh on Au(100) at 100 K; and (d)  $\sim 2$  ML of Rh grown on  $\sim 10$  ML Pd/Au(100) at 100 K and annealed at 450 K. All patterns were recorded at room temperature and at an electron-beam energy of  $\sim 66$  eV.